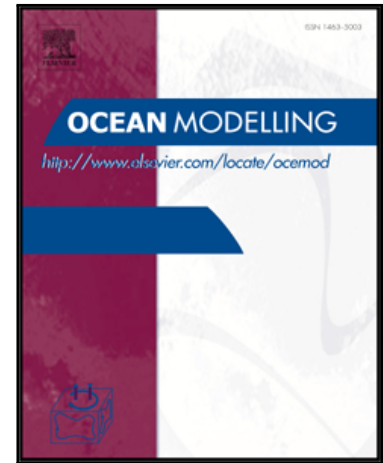


Accepted Manuscript

Emerging trends in the sea state of the Beaufort and Chukchi seas

Jim Thomson, Yalin Fan, Sharon Stammerjohn, Justin Stopa, W. Erick Rogers, Fanny Girard-Ardhuin, Fabrice Ardhuin, Hayley Shen, Will Perrie, Hui Shen, Steve Ackley, Alex Babanin, Qingxiang Liu, Peter Guest, Ted Maksym, Peter Wadhams, Chris Fairall, Ola Persson, Martin Doble, Hans Graber, Bjoern Lund, Vernon Squire, Johannes Gemmrich, Susanne Lehner, Benjamin Holt, Mike Meylan, John Brozena, Jean-Raymond Bidlot



PII: S1463-5003(16)30062-2
DOI: [10.1016/j.ocemod.2016.02.009](https://doi.org/10.1016/j.ocemod.2016.02.009)
Reference: OCEMOD 1120

To appear in: *Ocean Modelling*

Received date: 29 September 2015
Revised date: 18 February 2016
Accepted date: 29 February 2016

Please cite this article as: Jim Thomson, Yalin Fan, Sharon Stammerjohn, Justin Stopa, W. Erick Rogers, Fanny Girard-Ardhuin, Fabrice Ardhuin, Hayley Shen, Will Perrie, Hui Shen, Steve Ackley, Alex Babanin, Qingxiang Liu, Peter Guest, Ted Maksym, Peter Wadhams, Chris Fairall, Ola Persson, Martin Doble, Hans Graber, Bjoern Lund, Vernon Squire, Johannes Gemmrich, Susanne Lehner, Benjamin Holt, Mike Meylan, John Brozena, Jean-Raymond Bidlot, Emerging trends in the sea state of the Beaufort and Chukchi seas, *Ocean Modelling* (2016), doi: [10.1016/j.ocemod.2016.02.009](https://doi.org/10.1016/j.ocemod.2016.02.009)

This is a PDF file of an unedited manuscript that has been accepted for publication. As a service to our customers we are providing this early version of the manuscript. The manuscript will undergo copyediting, typesetting, and review of the resulting proof before it is published in its final form. Please note that during the production process errors may be discovered which could affect the content, and all legal disclaimers that apply to the journal pertain.

Highlights

- The seasonal extent of open water in the Arctic is increasing.
- The sea state is increasing in concert with the open water.
- Waves are larger and peak wave periods are longer.
- The additional wave energy is mostly directed at the coast (as opposed to the ice)

ACCEPTED MANUSCRIPT

Emerging trends in the sea state of the Beaufort and Chukchi seas

ONR Arctic Sea State DRI team:

Jim Thomson, Yalin Fan, Sharon Stammerjohn, Justin Stopa, W. Erick Rogers, Fanny Girard-Ardhuin, Fabrice Ardhuin, Hayley Shen, Will Perrie, Hui Shen, Steve Ackley, Alex Babanin, Qingxiang Liu, Peter Guest, Ted Maksym, Peter Wadhams, Chris Fairall, Ola Persson, Martin Doble, Hans Graber, Bjoern Lund, Vernon Squire, Johannes Gemmrich, Susanne Lehner, Benjamin Holt, Mike Meylan, John Brozena, and Jean-Raymond Bidlot

Correspondence: Jim Thomson, University of Washington, Applied Physics Laboratory, jthomson@apl.uw.edu, 206-616-0858

Abstract

The sea state of the Beaufort and Chukchi seas is controlled by the wind forcing and the amount of ice-free water available to generate surface waves. Clear trends in the annual duration of the open water season and in the extent of the seasonal sea ice minimum suggest that the sea state should be increasing, independent of changes in the wind forcing. Wave model hindcasts from four selected years spanning recent conditions are consistent with this expectation. In particular, larger waves are more common in years with less summer sea ice and/or a longer open water season, and peak wave periods are generally longer. The increase in wave energy may affect both the coastal zones and the remaining summer ice pack, as well as delay the autumn ice-edge advance. However, trends in the amount of wave energy impinging on the ice-edge are inconclusive, and the associated processes, especially in the autumn period of new ice formation, have yet to be well-described by in situ observations. There is an implicit trend and evidence for increasing wave energy along the coast of northern Alaska, and this coastal signal is corroborated by satellite altimeter estimates of wave energy.

Keywords: sea ice, Arctic Ocean, ocean surface waves

1 1. Introduction

2 The extent of seasonal sea ice in the Beaufort and Chukchi Sea of the
3 Arctic Ocean is changing (Jeffries et al., 2013). This paper explores the
4 timing and location of the annual ice minimum and transition to refreezing
5 conditions, with application to the sea state over the open water portion of
6 the domain. The sea state is set by the wind forcing, the open water fetch
7 distance available for wave generation, and the duration of time over which
8 the waves can accumulate energy from the wind. The wind forcing is episodic,
9 and thus best interpreted as probabilities for events (i.e., storms). The open
10 water distance, by contrast, has a much smoother signal that is dominated
11 by the seasonal retreat and advance of the sea ice. It is the combination of
12 these signals that determines the sea state of the Beaufort and Chukchi seas.

13 Trends in the Arctic sea ice have been examined by many previous stud-
14 ies (e.g., Wadhams, 1990; Wadhams and Davis, 2000; Stroeve et al., 2005,
15 2008; Simmonds and Keay, 2009; Kwok and Untersteiner, 2011). Meier et al.
16 (2013) show that in recent decades the Arctic sea ice cover has thinned and
17 become more seasonal, such that the total area covered is nearly 30% less
18 at the annual minimum than the corresponding mean from 1979 to 2000.
19 Stammerjohn et al. (2012) show that the duration of the summer open wa-
20 ter season since 1979 has become much longer in the Beaufort and Chukchi
21 seas due to an approximately 1.6 months earlier ice-edge retreat in spring,
22 followed by an approximately 1.4 month later ice-edge advance in autumn.
23 Stammerjohn et al. (2012) also find inter-annual links to the reduced ice
24 extent which are attributed to heat fluxes, especially increased duration of
25 summer solar heating, coupled with an overall thinner ice cover.

26 Coincident with the delay in the timing of the autumn ice advance, there is
27 a trend towards stronger autumn storms in recent years (Serreze et al., 1993,
28 2001; Zhang et al., 2004). The combination of these winds and increased
29 open water distances is expected to create high sea states (Francis et al.,
30 2011; Francis and Vavrus, 2012; Vermaire et al., 2013; Thomson and Rogers,
31 2014) and increase air-sea fluxes of heat and momentum, particularly in the
32 Beaufort and Chukchi seas (e.g., Simmonds and Keay, 2009). Some studies
33 have connected reduced ice cover with specific storm activity, such as in
34 August 2012 (Simmonds and Keay, 2012; Zhang et al., 2013; Parkinson and
35 Comiso, 2013). Of these, Parkinson and Comiso (2013) conclude that the
36 storm reduced the September ice extent minimum by an additional 5 percent.
37 This relatively small effect suggests that high sea states may be the result of

38 diminishing sea ice, but that high sea states are not yet the leading cause of
39 diminishing sea ice.

40 However, there is some evidence for feedbacks between ocean surface
41 waves and the loss of sea ice (e.g., Asplin et al., 2012). There are also
42 feedbacks between waves and ice formation, such as the rapid freezing that
43 occurs when waves cause pancake ice to develop (Wadhams et al., 1987;
44 Lange et al., 1989). Waves are both associated with the formation of pan-
45 cakes and attenuated by the pancakes, such that large areas of the ocean
46 can freeze quickly. Although this process is typically associated with the
47 Antarctic ice-edge or the Eastern Arctic, it is possible that this process will
48 become important in the Beaufort and Chukchi seas of the Western Arctic.
49 For example, this process is already common in the Sea of Okhotsk, which
50 is relatively sheltered.

51 Here, we set aside the many interesting questions of wave-ice interactions
52 (e.g., Squire et al., 1995; Squire, 2007) and focus instead on the large-scale
53 patterns of the sea state in the Beaufort and Chukchi seas. In particular, we
54 examine emerging trends in the probability of high sea states in the Beaufort
55 and Chukchi seas. The recent work of Wang et al. (2015) indicate the wave
56 heights are increasing slightly and wave periods are increasing strongly as a
57 result of reductions in ice cover (as opposed to changes in the winds). We
58 examine these trends and the autumn ice advance stage in particular. Section
59 2 describes the data products and model hindcasts used for the analysis.
60 Section 3 presents the results, using a full climatology of ice products and a
61 sub-set of wave hindcasts. Section 4 discusses the findings and corroborates
62 the coastal signal with satellite altimeter estimates of wave trends. Section
63 5 concludes.

64 **2. Methods**

65 Analysis of ice and sea state trends uses satellite products and model
66 hindcasts from an area-preserving domain shown in Figure 1. The domain
67 is a rectangle which is constant in area with latitude, such that the range
68 of longitudes included must expand northwards. The domain is selected to
69 cover the full extent of the seasonal variation in sea ice cover from the middle
70 of the summer (1 August) to the late autumn (31 October). The analysis
71 that follows uses this rectangle and is restricted to the months of August,
72 September, and October.

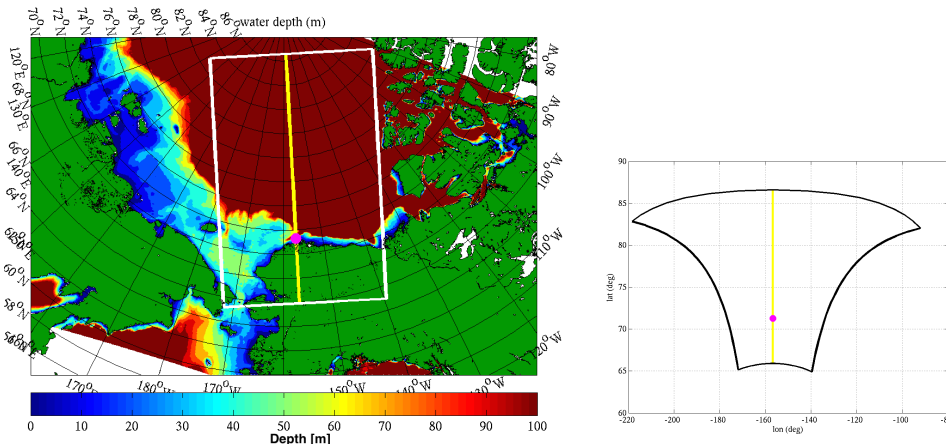


Figure 1: Region of analysis. (a) Map of bathymetry and the area-preserving rectangle defining the domain. Green colors show land. (b) Projection of the domain in latitude and longitude.

73 2.1. Sea ice satellite products

74 The analysis of sea ice area coverage used the NASA Goddard Space
 75 Flight Center (GSFC) Bootstrap SMMR-SSM/I Version 2 quasi-daily time
 76 series (1979 to 2014) of sea ice concentration from the EOS Distributed Active
 77 Archive Center (DAAC) at the National Snow and Ice Data Center (NSIDC,
 78 University of Colorado at Boulder, <http://nsidc.org>). The day of autumn
 79 ice advance and spring retreat is identified for each gridded (25 by 25 km
 80 pixel) location and for each sea ice year that begins/ends during the mean
 81 summer sea ice minimum (from mid-September to mid-September). When
 82 identifying day of ice-edge advance and retreat, an annual search window is
 83 defined such that it begins and ends during the mean summer sea ice extent
 84 minimum in mid-September. Within this interval, the year day of ice-edge
 85 advance is identified as when sea ice concentration first exceeds 15% (i.e., the
 86 approximate ice-edge) for at least five days. See Stammerjohn et al. (2012)
 87 and Comiso (2000, updated 2015, 2010) for further details.

88 Sea ice type was estimated by scatterometer, following Gohin and Cavanie
 89 (1994) and Girard-Ardhuin and Ezraty (2012), with the goal of examining
 90 trends in the relative amounts of first-year ice versus multi-year ice. The sea
 91 ice type results are similar using the Envisat altimeter, following Tran et al.
 92 (2009).

93 *2.2. Wind reanalysis product*

94 The wind and ice product used for wave hindcasting is ERA-Interim,
 95 which is a global reanalysis of recorded climate observations over the past 3.5
 96 decades (Dee, 2011). The spatial resolution of the data set is approximately
 97 80 km (T255 spectral) with 60 vertical levels from the surface up to 0.1 hPa,
 98 and the grid employed is 0.75 deg resolution. ERA-Interim is produced by
 99 the European Centre for Medium-Range Weather Forecasts (ECMWF). The
 100 temporal coverage is four time steps per day. The 10-m wind product is used
 101 to estimate the wind input to the wave model, following the latest source
 102 term formulation given in Ardhuin et al. (2010).

103 *2.3. Wave model hindcast*

104 Wave evolution, and thus the development of a sea state, is modeled by
 105 the Radiative Transfer Equation, as follows:

$$\frac{\partial E}{\partial t} + \nabla \cdot (\vec{c}_g E) = S_{\text{wind}} - S_{\text{brk}} + S_{\text{nl}} - S_{\text{ice}}, \quad (1)$$

106 where $E(\omega, \theta)$ is the directional wave energy spectrum and c_g is the group
 107 velocity (Masson and LeBlond, 1989; Young, 1999). The equation describes
 108 the temporal and spatial evolution of waves as an energy budget in fre-
 109 quency ω and direction θ . The deep-water source/sink terms are: input from
 110 the wind S_{wind} , dissipation via breaking S_{brk} , nonlinear interactions between
 111 wave frequencies S_{nl} , and interactions with sea ice S_{ice} . This is the basis
 112 of all contemporary, i.e., third-generation, wave prediction models. Here,
 113 we use the WAVEWATCH-III model of the US National Oceanographic and
 114 Atmospheric Administration (NOAA) (Tolman, 1991, 2009) with recent im-
 115 provements/options to the sea ice term S_{ice} (Rogers and Orzech, 2013) and
 116 a 16 km resolution polar stereographic grid (Rogers and Campbell, 2009)
 117 for the entire Arctic. The wave model also imports ice concentration fields
 118 from the ERA-interim, which are used to estimate the effects of sea ice on the
 119 waves using the Tolman (2003) scheme. Regions with concentration less than
 120 25% and greater than 75% are treated as open water and land respectively.
 121 Partial blocking is applied for intermediate ice concentrations.

122 The wave model hindcasts are performed for the minimum ice months
 123 (August, September, and October) for whole Arctic during the years span-
 124 ning 1992 to 2014. A more detailed analysis is conducted for the years 2004,
 125 2006, 2012, 2014. These four years bracket the modern ice conditions, and
 126 include 2012 as an extreme within the ‘new normal’.

127 Analysis of the wave model output within the defined Beaufort and Chukchi
 128 domain applies a threshold definition of ice concentrations less than 0.15 in
 129 defining “ice-free” areas. The percentage of the domain determined to be
 130 “ice-free” according to this threshold is tracked in time for each hindcast.
 131 Subsequent analyses use time series of spatial averages from the ice-free grid
 132 cells, in particular: total wave energy, $\int \int E d\theta d\omega$, the wave period at the
 133 peak of energy spectrum, T_p , and the wind stress, τ . Analyses also use his-
 134 tograms of the significant wave heights H_s from all ice-free grid cells and
 135 all time steps (i.e., no spatial or temporal averaging), with the conventional
 136 definition

$$\frac{1}{8} \rho g H_s^2 = \int \int E d\theta d\omega. \quad (2)$$

137 Finally, an evaluation of the large-scale potential of wave-ice interactions uses
 138 the normal component of wave energy flux incident to the ice-edge, given by

$$F = \int E \vec{c}_g \cdot \hat{n} d\theta, \quad (3)$$

139 where \hat{n} is the local unit vector normal to the ice-edge. The result is the
 140 total rate at which wave energy leaves the open water and enters the sea ice
 141 (i.e., the boundary of a control volume). Figure 2 shows an example of the
 142 model hindcast and application of Eq. 3.

143 2.4. Satellite altimeter

144 Additional wave products used are from satellite altimeters: the entire
 145 Envisat record (Queffelec and Croize-Fillon, 2012) and CRYOSAT altime-
 146 try from the NOAA Laboratory for Satellite Altimetry. The altimeter data
 147 were quality controlled and calibrated according to Zieger et al. (2009).

148 3. Results

149 3.1. Ice cover results

150 Trends in timing of ice advance were determined from the passive mi-
 151 crowave record over the period 1979-2014 using the method described in
 152 Stammerjohn et al. (2012). Over this span, the timing of the autumn ice ad-
 153 vance has become significantly later throughout the Arctic. Figure 3 shows
 154 a map of the rate of change, in days per year, for the date of the ice-edge ad-
 155 vance. The most pronounced change has been in the Beaufort and Chukchi

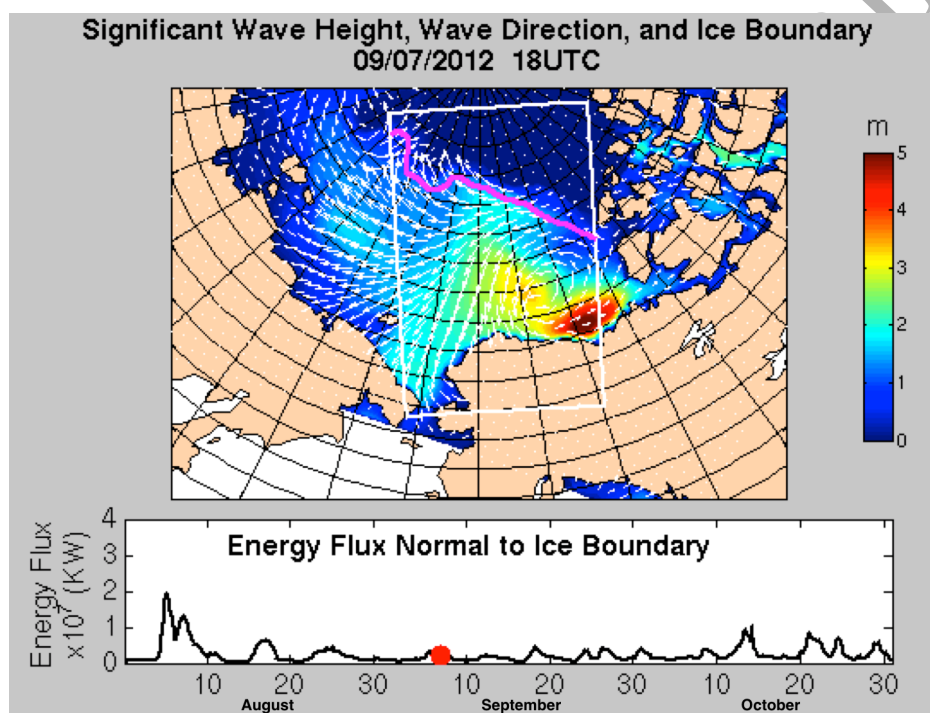


Figure 2: Example WAVEWATCH III hindcast showing significant wave heights (color scale), wave directions (white arrows), ice-edge (magenta curve), Beaufort-Chukchi domain (white outline box), and ice-normal energy flux time series (lower panel). The red dot in the lower panel corresponds to the time of the wave height map.

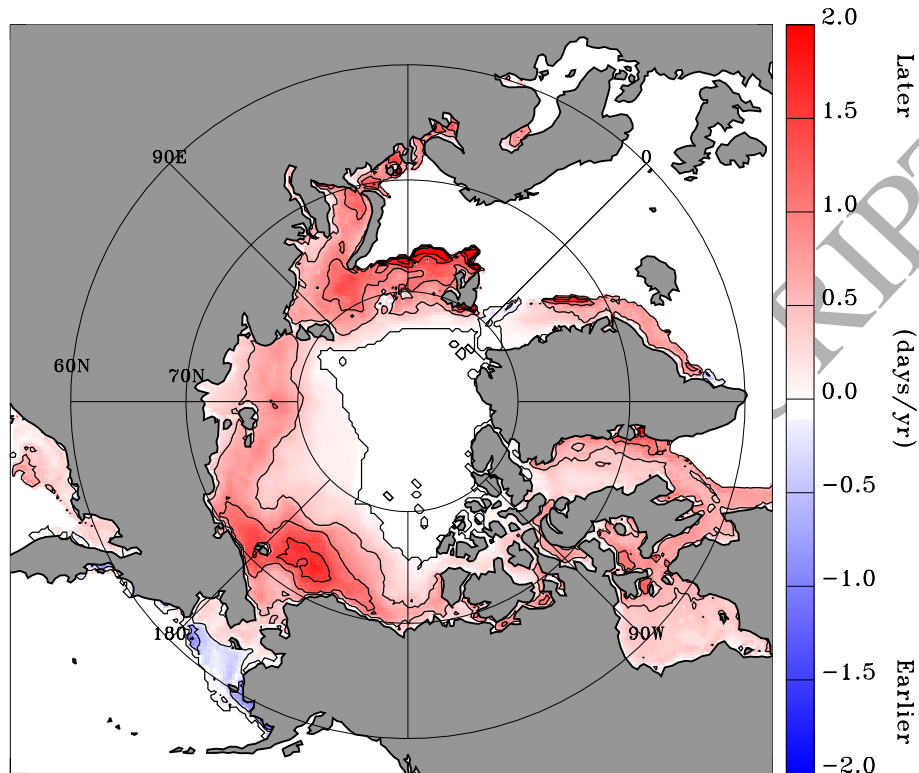


Figure 3: Average rate of change, in days per year (contours and colors), of the timing for the autumn ice advance in the Arctic. The most notable delay in ice advance is in the Beaufort and Chukchi seas (north of Alaska). Trends greater than ± 0.5 days per year are significant at the 0.01 level, with standard error determined using the effective degrees of freedom present in the regression residuals.

156 seas, where the statistically significant trend is 1.4 days later per year, with
 157 a similar trend towards earlier open-water in the spring. The trend is par-
 158 ticularly strong near the northern coast of Alaska and the Chukchi shelf,
 159 where recent years have almost an additional 3 months of open water from
 160 the spring to the autumn (relative to previous decades).

161 The inter-annual variability of this signal is shown in Figure 4, which
 162 uses a spatial average of the ice-advance date over the defined Beaufort-
 163 Chukchi domain. The ice advance date is simply the day of the year that
 164 the ice covered portion of the domain begins to increase. The linear trend
 165 is: 0.41 ± 0.07 days per year. Note however, that the trend over the whole

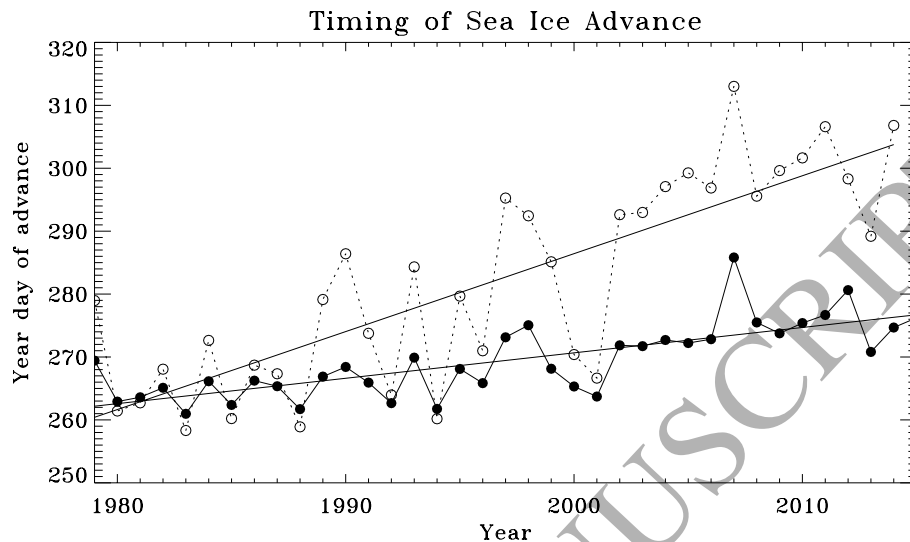


Figure 4: Spatial average for the date in the autumn when sea ice begins to refreeze and advance southwards, by year. The solid black line is the average over the entire Beaufort and Chukchi domain. The gray dashed line is the average within the coastal perimeter of the domain. The trends are shown as thin lines.

166 domain is modest compared with the coastal portion of the domain (where
 167 the average trend is 1.2 ± 0.2 days per year. Although 2012 was the minimum
 168 ice extent by area, 2007 is actually the latest timing for autumn ice advance
 169 in the record.

170 The changes in timing and ice area are likely related to the loss of multi-
 171 year ice. Ice type for the years 1999 to 2009 (using QuikSCAT) and 2008
 172 to 2015 (using ASCAT) is shown in Figure 5. As seen, in the domain with
 173 which we are concerned, the extent of multi-year has decreased, with the
 174 most dramatic retreat in the period from 2005 to 2009. Simultaneously, the
 175 extent of the first year ice features an upward trend. Similar results can
 176 also be found in Maslanik et al. (2007, 2011). Based on satellite measure-
 177 ments, these authors concluded that the sea ice in the Arctic is becoming
 178 younger and thinner, represented by the extensive loss of perennial multi-
 179 year ice. Similarly, the long-term reduction in sea ice thickness in the Arctic
 180 was clearly identified by Kwok and Rothrock (2009) using a combination of
 181 submarine- and satellite-derived thickness measurements.

182 Both the spatial view of the overall trend (Figure 3) and the temporal
 183 view averaged over the domain (Figure 4) indicate that in recent years the

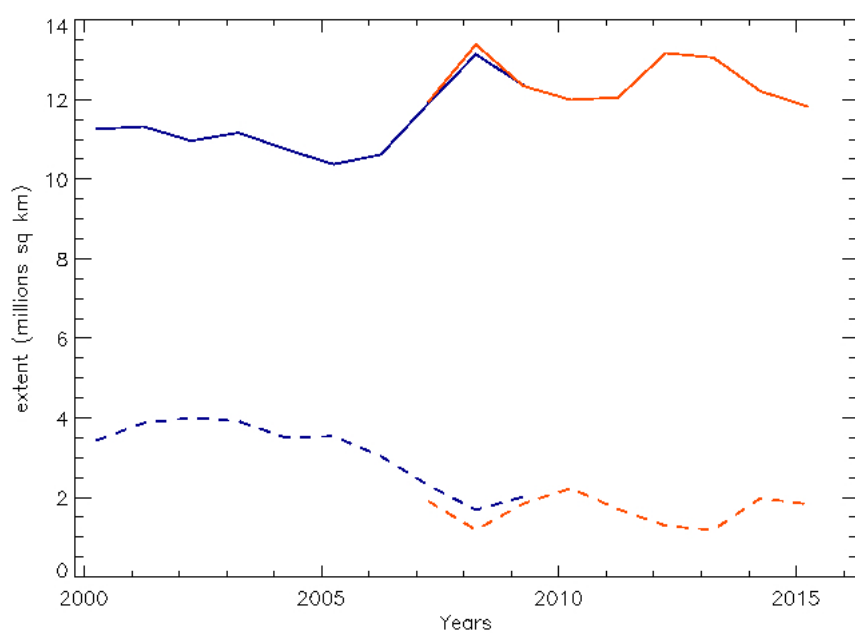


Figure 5: Multi year (solid line) and first year (dotted line) sea ice extents estimate in the Arctic for March since 2000 using satellite scatterometers. QuikSCAT sensor estimates are in blue, ASCAT results are in red (Ifremer/CERSAT).

184 Beaufort-Chukchi domain has more space and time with open water in the
185 autumn. Coupled with the known pattern of strong winds in the autumn,
186 the logical expectation is for the sea state to increase.

187 *3.2. Sea state results*

188 The relationship between the changing autumn ice advance and the sea
189 state is evaluated using wave model hindcasts of the late summer and autumn
190 from four years that span recent ice conditions. The 2004, 2006, and 2014 ice
191 conditions are used as “typical” years, and 2012 is used as an extreme year
192 (with minimal ice extent and delayed ice advance). This extreme year (2012)
193 had anomalously high air and sea surface temperatures during the autumn
194 months, and this likely contributed to the observed delay in the ice-edge
195 advance relative to other years.

196 Figure 6 shows the time series of area-averaged ice and sea state quantities
197 from these hindcasts. The percent of ice free area in the domain (panel a) is
198 a relatively smooth quantity in time, because of area-averaging. In contrast,
199 the sea state quantities of wave energy, peak period, and wind stress (panels
200 b, c, and d, respectively) have high variability, because the sea state is event-
201 driven and the autumn storms often encompass much of the domain (such
202 that area-averaging does not smooth the signal).

203 The evolution of ice-free area for the four hindcast years is consistent
204 with the timing of autumn ice advance (Figure 4), although it is interesting
205 to note that 2006 has a similar ice-advance to 2004 and 2014, despite much
206 less ice-free area in the late summer. The ice free area and the delay in ice
207 advance are both notably larger for 2012 than the other years. This means
208 more time and space were available for the generation of waves, given a set
209 of wind forcing conditions. However, the time series of wave energy, peak
210 period, and wind stress are not noticeably different between 2012 and the
211 other hindcast years. Indeed, the ‘Great Arctic Cyclone’ of August 2012 is
212 hardly evident in this analysis. All years show a consistent increase in winds
213 and waves into the autumn. The largest event energy is actually from the
214 year with the least ice-free area (2006), though it did have the strongest wind
215 event, as described below. This event was an intense storm near the coast
216 of Alaska, with hindcast 26 m/s maximum winds and 8 m significant wave
217 height. This highlights the importance of wind forcing in determining the
218 sea state, even with large variations in ice-free area. Since the area-averaged
219 wind is not noticeably different between the different years (other than the

220 particular storm of Oct 2006), it is not surprising that the area-averaged
221 waves are not noticeably different.

222 However, the event-driven nature of the sea state is best examined proba-
223 bilistically. Histograms and fitted Weibull probability distribution functions
224 are used to identify differences, and this is where the effect of a low summer
225 ice extent minimum followed by a late ice-edge advance in autumn in 2012 is
226 very apparent. Using the whole domain and all time steps of the hindcasts
227 addresses probability of a given sea state anywhere in the domain, with an
228 explicit dependence on ice cover. Restricting the analysis to ice-free grid cells
229 addresses the probability of a given sea state anywhere there is open water,
230 with an implicit dependence on ice cover. In the figures that follow, results
231 from both the whole domain and the ice-free portion are presented.

232 Figure 7 shows normalized histograms of significant wave heights and
233 fitted probability distribution functions for each year using all points in the
234 domain. The results are skewed by the high number of points with sea ice
235 cover (and thus zero or negligible wave heights). The 2012 distribution differs
236 from the other years, with a higher mean ($\langle H_s \rangle \sim 0.6$ m versus $\langle H_s \rangle \sim 0.3$
237 m) and longer tail. For example, the 2012 results have an almost 10% chance
238 of 2 m waves at any grid cell, compared with a 1% chance of this wave height
239 in the other years.

240 Figure 8 shows normalized histograms of significant wave heights and fit-
241 ted probability distribution functions for each year using only ice-free points
242 in the domain. The ice-free results across the different years are more similar
243 than the full domain results, but 2012 still shows the largest mean and high-
244 est probability of larger waves (except in the very tail of the distributions,
245 where limited sample sizes make differences statistically insignificant).

246 Figure 9 shows normalized histograms of peak wave period and fitted
247 probability distribution functions using only ice-free points in the domain.
248 Consistent with the results of Wang et al. (2015) and the expectations of
249 wave maturity over larger distances, there is a shift to longer period waves
250 for 2012. More striking, however, is the distribution for 2006, which is the
251 year with much less ice-free area but similar ice-advance timing to 2004 and
252 2014. The average 2006 peak wave period is shorter and the distribution of
253 peak wave periods is wider. This suggests that open water area may be more
254 important than the length of the open water season in determining sea state,
255 since the area difference for a year like 2006 persists throughout the whole
256 season and applies to multiple storm events (whereas a delay in ice advance
257 might only be relevant to the wave evolution of a single storm). For all years,

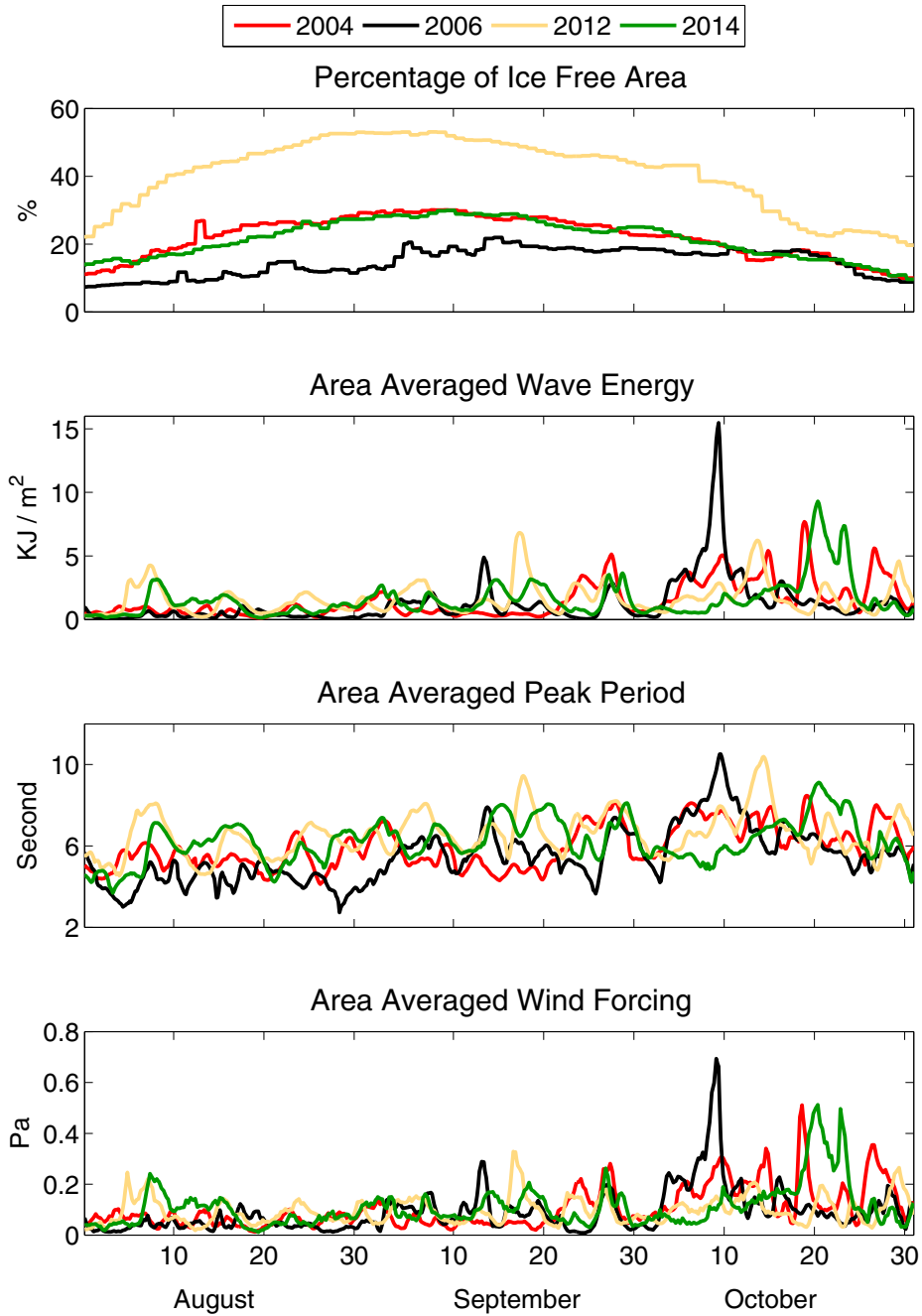


Figure 6: Time series of spatial averages over the Beaufort and Chukchi Sea in hindcasts of four selected years: (a) open water fraction, (b) wave energy, (c) wave peak period, (d) wind stress.

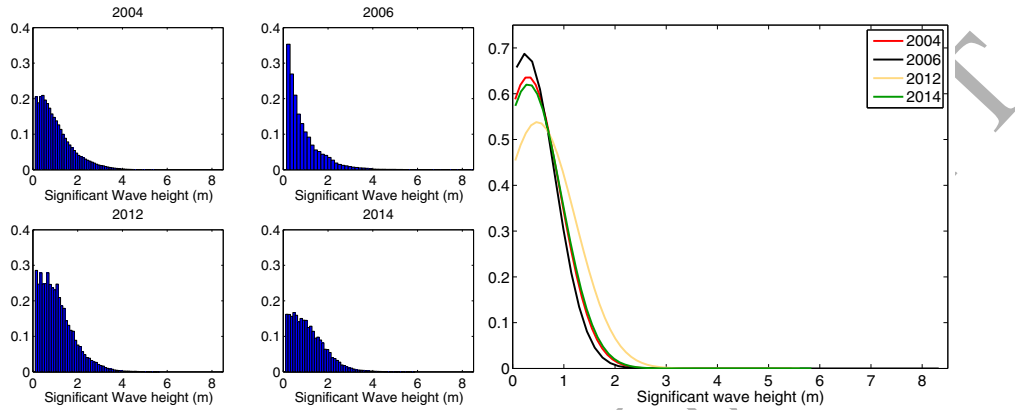


Figure 7: Normalized histograms of the significant wave height at all grid cells and all time steps for each of the hindcast years. Normalized probability distribution functions for significant wave height at all grid cells for each of the hindcast years.

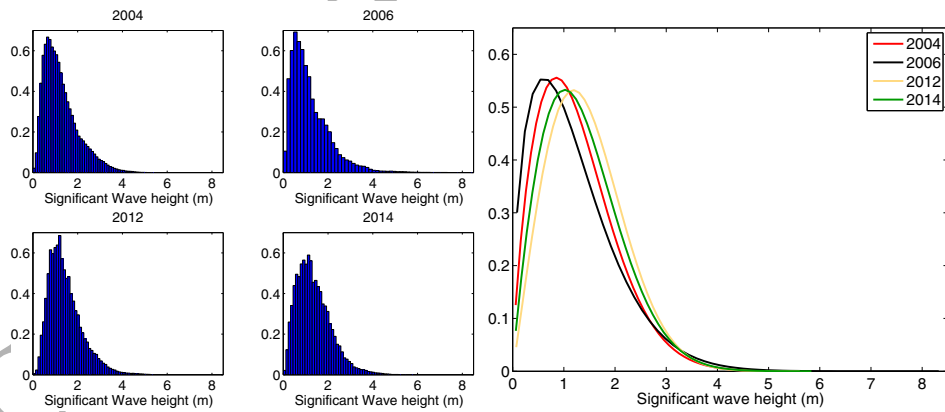


Figure 8: Normalized histograms of the significant wave height at all ice free grid cells and all time steps for each of the hindcast years. Normalized probability distribution functions for significant wave height at all ice free grid cells for each of the hindcast years.

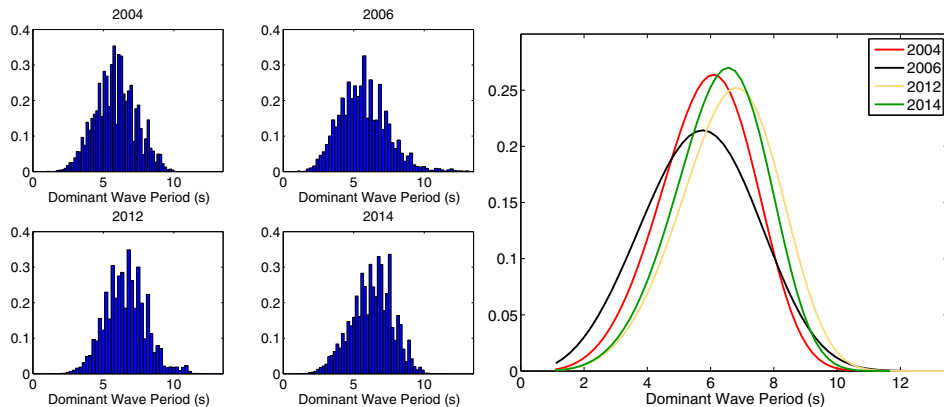


Figure 9: Normalized histograms of the peak wave period at all ice free grid cells and all time steps for each of the hindcast years. Normalized probability distribution functions for peak wave period at all ice free grid cells for each of the hindcast years.

258 the wave periods are still short ($T_p \sim 6$ s) relative to other oceans, indicating
 259 that, despite the emergence of swell in the Beaufort-Chukchi domain (e.g.,
 260 Thomson and Rogers, 2014), the sea state of any given ice-free location in
 261 the domain is still dominated by local wind waves.

262 Returning to the question of wind forcing, Figure 10 shows normalized
 263 histograms of wind speed and fitted probability distribution functions using
 264 only ice-free points in the domain. Although there are minor difference in the
 265 mean wind speeds, the storm winds that drive high sea states (> 10 m/s) are
 266 not significantly different. This is consistent with Wang et al. (2015), who
 267 find that variations in wind forcing are insufficient to explain the trends in
 268 the waves.

269 To examine the complete signal, wave model hindcasts for every year
 270 from 1992 to 2014 are analyzed following the same fitted Weibull probability
 271 distribution function analysis used for the four years examined in detail.
 272 Figure 11 shows the Weibull scale and shape parameters for significant wave
 273 height, peak period, and wind speed. The scale is used as a proxy for the
 274 mean value and the shape is used as a proxy for the standard deviation around
 275 that mean. There are statistically significant trends at the 95% level for both
 276 wave height and peak period, but not for wind speed. The peak period signal
 277 is particularly important, since most wave-ice interaction studies have found a
 278 strong dependence of wave attenuation on wave period. Following Wadhams
 279 et al. (1988), the trends in Figure 11 imply an increasing penetration scale

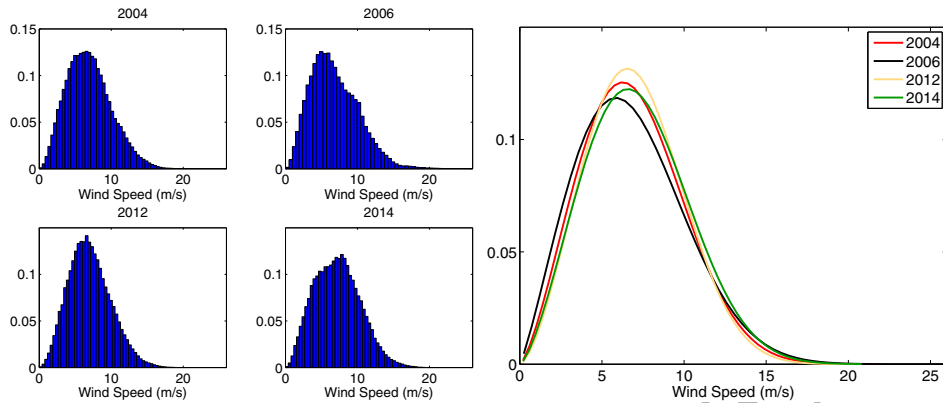


Figure 10: Normalized histograms of the wind speed at all ice free grid cells and all time steps for each of the hindcast years. Normalized probability distribution functions for wind speed at all ice free grid cells for each of the hindcast years.

280 for waves entering the sea ice, such that longer-period waves are expected to
 281 propagate several kilometers into the ice under recent conditions.

282 4. Discussion

283 It is logical that larger ice-free areas, which are persisting longer into the
 284 autumn, will result in higher sea states occurring more often in the Beaufort
 285 and Chukchi seas. The wave hindcasts presented here support this prediction,
 286 and the robustness of the result lies in the distinctness of the mechanism: all
 287 that is required to increase the probability of higher sea states is more ice-free
 288 area, and secondly, longer ice-free duration, not more storms or increased
 289 wind forcing. A compounding mechanism is storm duration: if storms of
 290 similar magnitude simply persist longer over open water, the resulting waves
 291 will be more mature and carry more energy flux.

292 The impact of an elevated autumn sea state on the overall Arctic system is
 293 difficult to determine without detailed understanding of wave-ice interactions,
 294 coastal impacts, and changes to fluxes across the air-sea-ice boundary. This is
 295 further complicated by the event-driven nature of the processes. A simplistic
 296 approach to the wave-ice question is to examine the total wave energy flux
 297 incident on the ice (Eq. 3). This is distinct from the question of overall wave
 298 activity (and associated air-sea fluxes), because an elevated sea state in the
 299 region does not affect the ice unless the waves reach the ice. Paradoxically,

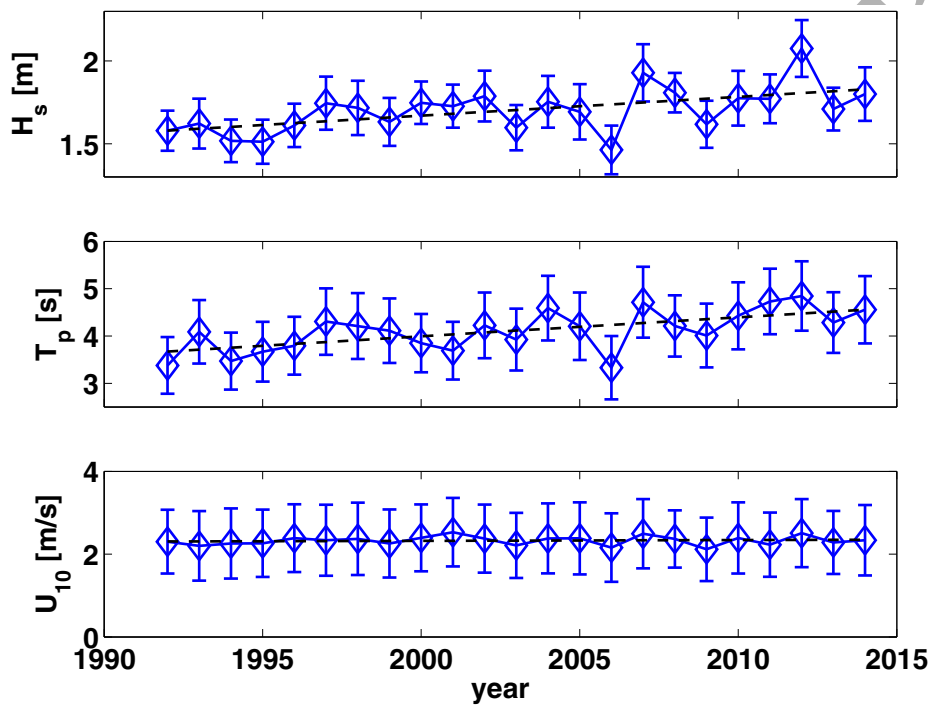


Figure 11: Trends in the Weibull fit parameters for significant wave height, peak period, and wind speed over the wave hindcast years. Diamonds are the scale parameter and the vertical bounded lines are the 95% confidence intervals of the shape parameter divided by a factor of ten (for visual simplicity). The black dashed lines are the estimated trend lines of the scale parameter. The significant wave height scale has a trend of 0.01 m increase per year and the peak period scale has a trend of 0.04 s increase per year, both of which are statistically significant at 95% confidence. The wind speed scale does not have a significant trend.

300 as the ice-free regions expand, there is more room for localized storms that
301 are far from the ice and may not directly affect the ice.

302 Figure 12 shows time series of the total integrated wave energy flux ar-
303 riving at the ice-edge. Similar to the energy results (Figure 6), the values
304 are similar across the years and generally increase later in the autumn. This
305 suggests that waves may be more important as a mechanism to alter ice ad-
306 vance (via the formation of pancakes, etc) in the autumn, rather than as a
307 mechanism to alter ice retreat (via fracturing) in the summer. This is, of
308 course, related to the increased ice-free area for wave generation in the au-
309 tumn. The present results are inconclusive in terms of trends in wave energy
310 flux arriving at the ice-edge. Although 2012 had more wave activity through-
311 out the domain, the overall rate of wave energy arriving at the ice-edge was
312 similar to other years. Still, the August 2012 storm is notable and waves
313 may have enhanced the well-documented effect of the storm on the rest of
314 that year (e.g., Parkinson and Comiso, 2013). Such feedbacks and the role of
315 wave directionality are the focus of forthcoming publications, such as Stopa
316 et al. (submitted).

317 Given that wave energy flux is a conserved quantity, with only minimal
318 dissipation occurring as waves propagate in open water (e.g., Ardhuin et al.,
319 2010), the increased wave energy inside the domain during the 2012 season
320 can be assumed to increase the flux along the other boundary: the northern
321 coast of Alaska. The satellite altimeter results in Figure 13 corroborate this
322 suggestion. Figure 13 shows a statistically significant increase in wave en-
323 ergy along the coast from 2007 onward, compared with no significant trend
324 (and an apparent slight decrease) in the wave energy along the ice-edge. The
325 satellite altimeter product is scalar energy only, and thus it is not possible
326 to calculate wave energy flux (Eq. 3) for a direct comparison and reconcili-
327 ation with the wave model hindcasts. Moreover, the satellite product is not
328 uniformly sampled and is poorly suited to the Weibull distribution fitting
329 that was used to identify trends in the preceding sections. We thus rely on
330 the model hindcasts for overall trends in the wave climate and discount the
331 non-significant trend in the altimeter analysis.

332 This implication for increasing wave energy along the coast is significant,
333 given the highly erodible nature of this coastline (Overeem et al., 2011).
334 Furthermore, this would suggest that winds are preferentially directed off-ice.
335 If so, wind-wave generation in partial ice cover may become more important
336 in the future Arctic, when the seasonal marginal ice zone is expected to be
337 more expansive. The process of wind-wave generation in partial ice cover is

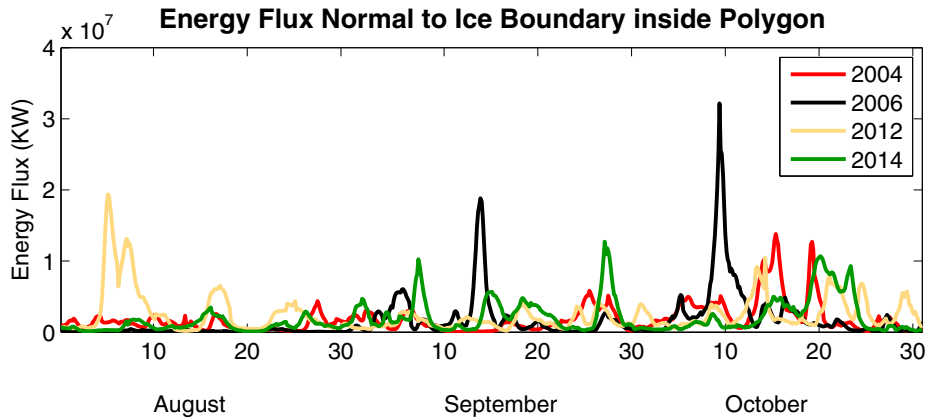


Figure 12: Time series of the total energy flux incident (normal component) to the ice-edge within the Beaufort and Chukchi seas for the hindcast years.

338 likely far more complex than present models suggest (Li et al., 2015; Zippel
339 and Thomson, 2016) and is in acute need of improved understanding.

340 5. Conclusion

341 The autumn storms that regularly occur in the Beaufort and Chukchi
342 Seas are likely elevating the sea state now, and will continue so into the
343 future, simply because it is increasingly likely that the storms will occur
344 over larger open water areas that persist longer into autumn. It is yet to be
345 determined if the higher sea states will in turn feed back to the large-scale
346 evolution of the sea ice. The increasing sea state may affect not only the ice
347 cover development, but also wave forcing in the coastal zone. Either way,
348 the increasing sea states may alter air-sea fluxes and associated ecosystem
349 processes. It is possible that the increasing sea state may play an important
350 role in modulating the presumed changes in air-sea fluxes and upper ocean
351 properties that are occurring, and in turn may modulate the response of sea
352 ice to climate change. Finally, higher sea states are of operational importance
353 to mariners and seabed drilling operators in the region, for whom higher sea
354 states can increase the likelihood of dangerous icing conditions on ships and
355 structures.

356 New observational data has just been collected to assess many of these
357 processes: the Office of Naval Research “Arctic Sea State and Boundary
358 Layer Physics” program (Thomson et al., 2013) followed the ice-edge advance

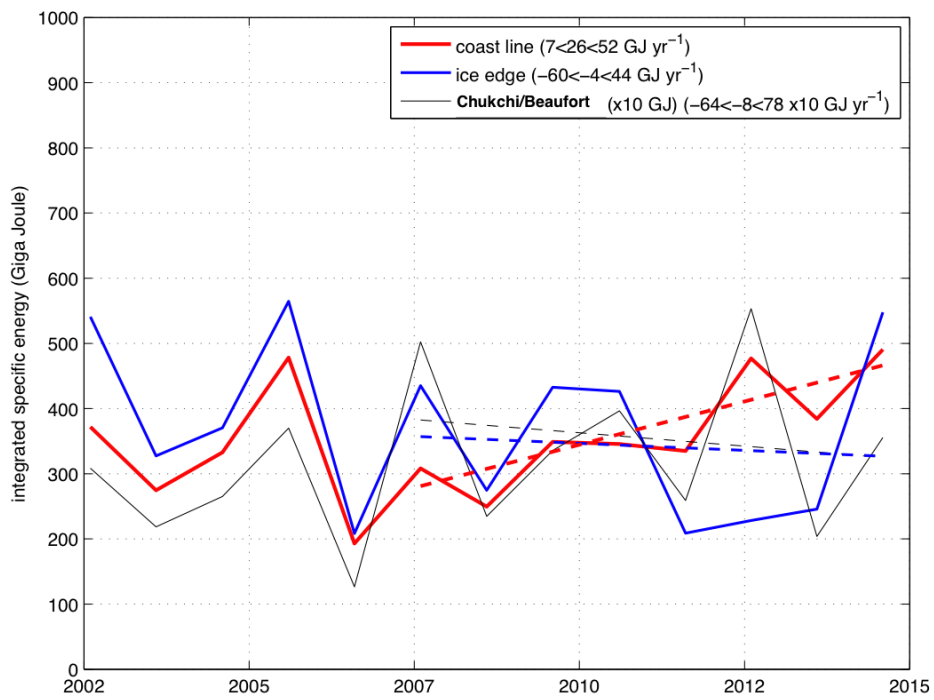


Figure 13: Yearly results from satellite altimetry estimates of spatially averaged wave energy along the northern coast of Alaska (red), along the ice-edge (blue), and over the entire domain (grey). Dashed lines show calculated trends.

359 during autumn 2015 while simultaneously sampling in situ air-sea-ice inter-
360 actions from the R/V Sikuliaq and multiple autonomous platforms. Pancake
361 ice associated with wave forcing was ubiquitous during the field campaign,
362 and the importance of this ice type is assumed to be increasing with the wave
363 climate in the region. The Sikuliaq cruise report and related information are
364 available at <http://www.apl.uw.edu/arcticseastate>.

365 Such process studies are essential to constrain the imperfect, yet neces-
366 sary, parameterizations used in climate models. Climate predictions for the
367 Beaufort-Chukchi domain already indicate that the expansion of seasonal
368 open water will only accelerate in the coming decades. Figure 14 shows
369 one such example of the predicted dramatic decrease in ice volume through
370 the autumn, using coupled ice-ocean model following the IPCC AR4 climate
371 change scenario A1B and results from Long and Perrie (2013, 2015). These
372 ice predictions are consistent with AR5 results following the recent work of
373 Wang and Overland (2015). Incorporating the feedbacks associated with a
374 changing sea state may significantly alter these predictions, but that remains
375 a speculation until the processes can be quantified and applied within the
376 climate models.

377 6. Acknowledgments

378 This work relies heavily on publicly available datasets, including those
379 from the US National Snow and Ice Data Center, the Canadian Space Agency,
380 and the European Centre for Medium-range Weather Forecasts. This work
381 was supported by the Office of Naval Research, Code 322, “Arctic and Global
382 Prediction”, directed by Drs. Martin Jeffries and Scott Harper. (Grant
383 numbers and Principal Investigators are: Ackley, N000141310435; Babanin,
384 N000141310278; Doble, N000141310290; Fairall, N0001413IP20046; Gemm-
385 rich, N000141310280; Graber, N000141310288; Guest, N0001413WX20830;
386 Holt, N0001413IP20050; Lehner, N000141310303; Maksym, N000141310446;
387 Perrie, N00014-15-1-2611; Rogers, N0001413WX20825; Shen, N000141310294;
388 Squire, N000141310279; Stammerjohn, N000141310434; Thomson, N000141310284;
389 Wadhams, N000141310289.)

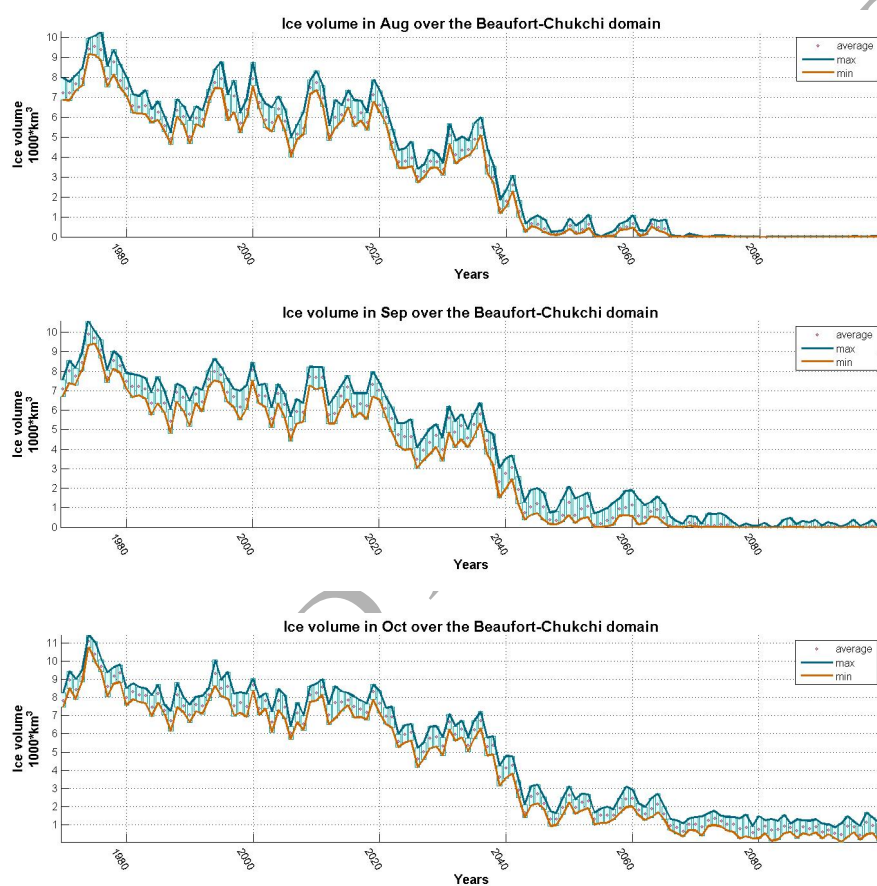


Figure 14: Estimates for ice volume in the Beaufort-Chukchi domain for 1970-2100 in the months of August, September and October using coupled ice-ocean model following the IPCC AR4 climate change scenario A1B.

390 **References**

- 391 Arduin, F., Rogers, W., Babanin, A., Filipot, J.-F., Magne, R., Roland, A.,
 392 van der Westhuysen, A., Queffelec, P., Lefevre, J.-M., Aouf, L., Collard,
 393 F., 2010. Semi-empirical dissipation source functions for ocean waves: Part
 394 I, definitions, calibration, and validations. *J. Phys. Oceanogr.* 40, 1917–
 395 1941.
- 396 Asplin, M. G., Galley, R., Barber, D. G., Prinsenberg, S., 2012. Fracture of
 397 summer perennial sea ice by ocean swell as a result of Arctic storms. *J.*
 398 *Geophys. Res.* 117 (C06025).
- 399 Comiso, J. C., 2000, updated 2015. Bootstrap sea ice concentrations
 400 from Nimbus-7 SMMR and DMSP SSM/I-SSMIS. version 2. NASA Na-
 401 tional Snow and Ice Data Center Distributed Active Archive Center.
 402 <http://dx.doi.org/10.5067/J6JQLS9EJ5HU>.
- 403 Comiso, J. C., 2010. *Polar Oceans from Space*. Springer, New York.
- 404 Dee, D. P., 2011. The era-interim reanalysis: configuration and performance
 405 of the data assimilation system. *Quart. J. Roy. Meteor. Soc.* 137 (656),
 406 553–597.
- 407 Francis, J. A., Vavrus, S. J., 2012. Evidence linking Arctic amplification to
 408 extreme weather in mid-latitudes. *Geophysical Research Letters* 39 (6),
 409 n/a–n/a.
 410 URL <http://dx.doi.org/10.1029/2012GL051000>
- 411 Francis, O. P., Panteleev, G. G., Atkinson, D. E., 2011. Ocean wave condi-
 412 tions in the Chukchi Sea from satellite and in situ observations. *Geophys.*
 413 *Res. Lett.* 38 (L24610).
- 414 Girard-Arduin, F., Ezraty, R., 2012. Enhanced arctic sea ice drift estimation
 415 merging radiometer and scatterometer data. *IEEE Trans. Geosci. Remote*
 416 *Sensing* 50 (7), 2639–2648.
- 417 Gohin, F., Cavanie, A., 1994. A first try at identification of sea ice using the
 418 three beam scatterometer of ers-a. *Int. J. Remote Sensing* 15 (6), 1221–
 419 1228.
- 420 Jeffries, M. O., Overland, J. E., Perovich, D. K., 2013. The Arctic shifts to
 421 a new normal. *Physics Today* 66 (10).

- 422 Kwok, R., Rothrock, D. A., 2009. Decline in Arctic sea ice thickness from sub-
423 marine and ICESat records: 1958–2008. *Geophys. Res. Lett.* 36 (L15501).
- 424 Kwok, R., Untersteiner, N., April 2011. The thinning of Arctic sea ice.
425 *Physics Today*, 36–41.
- 426 Lange, M., Ackley, S., Wadhams, P., Dieckmann, G., Eicken, E., 1989. De-
427 velopment of sea ice in the Weddell sea. *Annals of Glaciology* 12.
- 428 Li, J., Kohout, A. L., Shen, H. H., 2015. Comparison of wave propagation
429 through ice covers in calm and storm conditions. *Geophysical Research*
430 *Letters* 42 (14), 5935–5941, 2015GL064715.
431 URL <http://dx.doi.org/10.1002/2015GL064715>
- 432 Long, Z., Perrie, W., 2013. Impacts of climate change on fresh water content
433 and sea surface height in the Beaufort Sea. *Ocean Modelling* 71, 127–139.
- 434 Long, Z., Perrie, W., 2015. Scenario changes of Atlantic water in the Arctic
435 Ocean. *J. Climate* 28, 552305548.
- 436 Maslanik, J. A., Fowler, C., Stroeve, J. C., Drobot, S., Zwally, J., Yi, D.,
437 Emery, W., 2007. A younger, thinner Arctic ice cover: Increased potential
438 for rapid, extensive sea-ice loss. *Geophys. Res. Lett.* 34 (34).
- 439 Maslanik, J. A., Stroeve, J. C., Fowler, C., Emery, W., 2011. Distribution
440 and trends in Arctic sea ice age through spring 2011. *Geophys. Res. Lett.*
441 38 (13), 2–7.
- 442 Masson, D., LeBlond, P., 1989. Spectral evolution of wind-generated surface
443 gravity waves in a dispersed ice field. *J. Fluid Mech.* 202 (111).
- 444 Meier, W., Gallaher, D., Campbell, G. G., 2013. New estimates of Arctic and
445 Antarctic sea ice extent during september 1964 from recovered Nimbus I
446 satellite imagery. *The Cryosphere* 7, 699–705.
- 447 Overeem, I., Anderson, R. S., Wobus, C. W., Clow, G. D., Urban, F. E.,
448 Matell, N., 2011. Sea ice loss enhances wave action at the Arctic coast.
449 *Geophysical Research Letters* 38 (17), n/a–n/a.
450 URL <http://dx.doi.org/10.1029/2011GL048681>

- 451 Parkinson, C. L., Comiso, J. C., 2013. On the 2012 record low Arctic sea ice
452 cover: Combined impact of preconditioning and an August storm. *Geo-*
453 *physical Research Letters* 40, 1356–1361.
- 454 Queffeuilou, P., Croize-Fillon, D., 2012. Global altimeter SWH data set. Tech-
455 nical Report Version 9, Laboratoire d’Oceanographie Spatiale IFREMER,
456 Plouzanne, France.
- 457 Rogers, W., Campbell, T. J., 2009. Implementation of curvilinear coordi-
458 nate system in the WAVEWATCH-III model. NRL Memorandum Report
459 NRL/MR/7320-09-9193, Naval Research Laboratory.
- 460 Rogers, W., Orzech, M. D., 2013. Implementation and testing of ice
461 and mud source functions in WAVEWATCH III. Memorandum Report
462 NRL/MR/7320-13-9462, Naval Research Laboratory.
463 URL <http://www7320.nrlssc.navy.mil/pubs.php>
- 464 Serreze, M. C., Box, J. E., Barry, R. G., Walsh, J. E., 1993. Characteristics
465 of Arctic synoptic activity. *Met. Atmos. Phys.* 51, 147–164.
- 466 Serreze, M. C., Lynch, A. H., Clark, M. P., 2001. The summer Arctic frontal
467 zone as seen in the NCEP/NCAR reanalysis. *J. Climate* 14, 1550–1567.
- 468 Simmonds, I., Keay, K., 2009. Extraordinary September arctic sea ice reduc-
469 tions and their relationships with storm behavior over 1979-2008. *Geophys.*
470 *Res. Lett.* 36 (L19715).
- 471 Simmonds, I. K., Keay, K., 2012. The great Arctic cyclone of August 2012.
472 *Geophys. Res. Lett.* 39 (L23709).
- 473 Squire, V. A., 2007. Of ocean waves and sea ice revisited. *Cold Regions Sci.*
474 *Tech.* 49, 110–133.
- 475 Squire, V. A., Dugan, J. P., Wadhams, P., Rottier, P. J., Liu, A. K., 1995.
476 Of ocean waves and sea ice. *Annu. Rev. Fluid Mech.* 27, 115–168.
- 477 Stammerjohn, S., Massom, R., Rind, D., Martinson, D., 2012. Regions of
478 rapid sea ice change: An inter-hemispheric seasonal comparison. *Geophys-*
479 *ical Research Letters* 39 (6), n/a–n/a, 106501.
480 URL <http://dx.doi.org/10.1029/2012GL050874>

- 481 Stopa, J. E., Ardhuin, F., Girard-Adrhuin, F., submitted. Wave-climate in
482 the Arctic 1992-2014: seasonality, trends, and wave-ice influence. *The*
483 *Cryosphere*.
- 484 Stroeve, J., Serreze, M., Drobot, S., Gearheard, S., Holland, M., et al., 2008.
485 Arctic sea ice extent plummets in 2007. *Eos Trans. AGU* 89, 1314.
- 486 Stroeve, J. C., Serreze, M. C., Fetterer, F., Arbetter, T., Meier, W., 2005.
487 Tracking the Arctic's shrinking ice cover: Another extreme September
488 minimum in 2004. *Geophys. Res. Lett.* 32 (L04501).
- 489 Thomson, J., Rogers, W. E., 2014. Swell and sea in the emerging Arctic
490 Ocean. *Geophysical Research Letters*, n/a–n/a.
491 URL <http://dx.doi.org/10.1002/2014GL059983>
- 492 Thomson, J., Squire, V., Ackley, S., Rogers, E., Babanin, A., Guest, P.,
493 Maksym, T., Wadhams, P., Stammerjohn, S., Fairall, C., Persson, O.,
494 Doble, M., Graber, H., Shen, H., Gemrich, J., Lehner, S., Holt, B.,
495 Williams, T., Meylan, M., Bidlot, J., 2013. Science plan: Sea state and
496 boundary layer physics of the emerging Arctic Ocean. Technical Report
497 1306, Applied Physics Laboratory, University of Washington.
- 498 Tolman, H. L., 1991. A third generation model for wind-waves on slowly vary-
499 ing, unsteady, and inhomogeneous depths and currents. *J. Phys. Oceanogr.*
500 21 (6), 782–797.
- 501 Tolman, H. L., 2003. Treatment of unresolved islands and ice in wind wave
502 models. *Ocean Modeling* 5, 219–231.
- 503 Tolman, H. L., 2009. User manual and system documentation of WAVE-
504 WATCH III version 3.14. Tech. Rep. 276, NOAA/NWS/NCEP/Marine
505 Modeling and Analysis Branc, Camp Springs, MD (USA).
- 506 Tran, N., Girard-Adrhuin, F., Ezraty, R., Feng, H., Femenias, P., January
507 2009. Defining a sea ice flag for Envisat altimetry mission. *IEEE Geoscience*
508 *and Remote Sensing Letters* 6 (1), 77–81.
- 509 Vermaire, J. C., Pisaric, M. F. J., Thienpont, J. R., Courtney Mustaphi,
510 C. J., Kokelj, S. V., Smol, J. P., 2013. Arctic climate warming and sea
511 ice declines lead to increased storm surge activity. *Geophysical Research*

- 512 Letters 40 (7), 1386–1390.
513 URL <http://dx.doi.org/10.1002/grl.50191>
- 514 Wadhams, P., 1990. Evidence for thinning of the Arctic ice cover north of
515 Greenland. *Nature* 345 (795-797).
- 516 Wadhams, P., Davis, N. R., 2000. Further evidence of ice thinning in the
517 Arctic Ocean. *Geophys. Res. Lett.* 27 (24), 3973–3976.
- 518 Wadhams, P., Lange, M. A., Ackley, S. F., 1987. The ice thickness distri-
519 bution across the Atlantic sector of the Antarctic Ocean in midwinter. *J.*
520 *Geophys. Res* 92 (C13), 14535–14552.
- 521 Wadhams, P., Squire, V. A., Goodman, D. J., Cowan, A. M., Moore, S. C.,
522 1988. The attenuation rates of ocean waves in the marginal ice zone. *J.*
523 *Geophys. Res* 93 (C6), 6799–6818.
- 524 Wang, M., Overland, J., January 2015. Projected future duration of the sea-
525 ice-free season in the Alaskan Arctic. *Progress in Oceanography*.
- 526 Wang, X. L., Feng, Y., Swail, V. R., Cox, A., 2015/08/28 2015. Histori-
527 cal changes in the Beaufort-Chukchi-Bering seas surface winds and waves,
528 1971-2013. *Journal of Climate*.
529 URL <http://dx.doi.org/10.1175/JCLI-D-15-0190.1>
- 530 Young, I., 1999. *Wind Generated Ocean Waves*. Elsevier Ocean Engineering
531 Book Series. Elsevier, New York.
- 532 Zhang, J., Lindsay, R., Schweiger, A., Steele, M., 2013. The impact of an in-
533 tense summer cyclone on 2012 Arctic sea ice retreat. *Geophysical Research*
534 *Letters* 40 (4), 720–726.
535 URL <http://dx.doi.org/10.1002/grl.50190>
- 536 Zhang, X., Walsh, J., Zhang, J., Bhatt, U., Ikeda, M., 2004. Climatology and
537 interannual variability of Arctic cyclone activity: 1948-2002. *J. Climate*
538 17, 2300–2317.
- 539 Zieger, S., Vinoth, J., Young, I. R., 2009. Joint calibration of multi-platform
540 altimeter measurements of wind speed and wave height over the past 20
541 years. *J. Atmos. Ocean. Tech.* 26, 2549–2564.

542 Zippel, S., Thomson, J., 2016. Air-sea interactions in the marginal ice zone.
543 Elem Sci Anth 4 (000095).

ACCEPTED MANUSCRIPT